

University of Massachusetts Medical School
eScholarship@UMMS

Open Access Articles

Open Access Publications by UMMS Authors

2006-03-02


Targeting of C-terminal binding protein (CtBP) by ARF results in p53-independent apoptosis

Seema Paliwal
University of Massachusetts Medical School

Et al.

Let us know how access to this document benefits you.

Follow this and additional works at: <https://escholarship.umassmed.edu/oapubs>

 Part of the [Life Sciences Commons](#), and the [Medicine and Health Sciences Commons](#)

Repository Citation

Paliwal S, Pande S, Kovi RC, Sharpless NE, Bardeesy N, Grossman SR. (2006). Targeting of C-terminal binding protein (CtBP) by ARF results in p53-independent apoptosis. Open Access Articles. <https://doi.org/10.1128/MCB.26.6.2360-2372.2006>. Retrieved from <https://escholarship.umassmed.edu/oapubs/1410>

This material is brought to you by eScholarship@UMMS. It has been accepted for inclusion in Open Access Articles by an authorized administrator of eScholarship@UMMS. For more information, please contact Lisa.Palmer@umassmed.edu.

Targeting of C-Terminal Binding Protein (CtBP) by ARF Results in p53-Independent Apoptosis

Seema Paliwal,¹ Sandhya Pande,¹† Ramesh C. Kovi,¹† Norman E. Sharpless,⁴
Nabeel Bardeesy,⁵ and Steven R. Grossman^{1,2,3*}

Departments of Cancer Biology¹ and Medicine² and Gastrointestinal Cancer Program,³ University of Massachusetts Medical School and Cancer Center, Worcester, Massachusetts 01605; Departments of Medicine and Genetics, Lineberger Comprehensive Cancer Center, University of North Carolina, Chapel Hill, North Carolina 27599⁴; and MGH Cancer Center, Charlestown, Massachusetts 02129⁵

Received 14 July 2005/Returned for modification 16 August 2005/Accepted 23 December 2005

ARF encodes a potent tumor suppressor that antagonizes MDM2, a negative regulator of p53. ARF also suppresses the proliferation of cells lacking p53, and loss of ARF in p53-null mice, compared with ARF or p53 singly null mice, results in a broadened tumor spectrum and decreased tumor latency. To investigate the mechanism of p53-independent tumor suppression by ARF, potential interacting proteins were identified by yeast two-hybrid screen. The antiapoptotic transcriptional corepressor C-terminal binding protein 2 (CtBP2) was identified, and ARF interactions with both CtBP1 and CtBP2 were confirmed in vitro and in vivo. Interaction with ARF resulted in proteasome-dependent CtBP degradation. Both ARF-induced CtBP degradation and CtBP small interfering RNA led to p53-independent apoptosis in colon cancer cells. ARF induction of apoptosis was dependent on its ability to interact with CtBP, and reversal of ARF-induced CtBP depletion by CtBP overexpression abrogated ARF-induced apoptosis. CtBP proteins represent putative targets for p53-independent tumor suppression by ARF.

ARF (p19^{ARF} in mouse [mArf] and p14^{ARF} in human [hARF]) is a tumor suppressor product of the *INK4a/ARF* locus (34) that acts, in part, by stabilizing p53 (reviewed in reference 40). Germ line homozygous knockout of *Arf* in mice results in the development of highly penetrant lymphoma or sarcoma, a phenotype similar to that observed with p53-deficient mice (22, 39). Given the molecular observation that ARF stabilizes and activates p53 by antagonizing MDM2, ARF inactivation has been commonly viewed as one of many means of inactivating the p53 pathway, a sine qua non for mammalian tumorigenesis (27). Accordingly, ARF is frequently inactivated in human cancers by deletion, mutation, or transcriptional silencing (38). However, the finding of simultaneous p53 and *INK4a/ARF* inactivation in certain human tumors suggests that ARF may encode an additional tumor suppressor function(s) apart from the activation of p53 (35).

Given the difficulty of distinguishing the tumor suppressor contributions of the often concordantly regulated p16^{INK4a} and ARF genes in humans (38), analysis of *Arf*-specific knockout mice has provided additional evidence for p53-independent functions of ARF. Epithelial tumors are rare in p53 knockout mice but, depending on the study, are observed in about 12% to 28% of *Arf* knockout mice (21, 39). Further loss of p53 and/or the p53 and ARF antagonist *Mdm2* results in a substantially increased incidence of epithelial cancers, including those of the digestive tract (31, 48). In comparison, mice with loss of *p53* and *Mdm2* but retention of *Arf* display mainly

mesenchymal tumors, as do *p53* knockout mice (19, 30, 48). Moreover, in a transgenic K-ras skin cancer model, *Arf* loss accelerated tumor growth in a p53-independent manner (24). Thus, the genetic evidence in the mouse supports the existence of an ARF tumor suppressor activity that functions independently of p53.

At the cellular level, ARF can suppress the proliferation of p53-defective cells (48, 52). At least two mechanisms have been identified. First, under conditions of overexpression, ARF appears to bind and antagonize both *c-myc* and activator E2F proteins, the latter also being degraded via the proteasome, thus slowing progression of cells through the G₁/S transition and decreasing proliferative rate (10, 11, 28, 33). Second, ARF is concentrated in nucleoli, forming a stoichiometric complex with nucleophosmin/B23, disrupting ribosome biogenesis by interfering with the export of rRNA (2, 4, 18, 25, 41). This, in turn, would be predicted to hamper progression of cells through the growth phases of the cell cycle.

The actual mechanism by which ARF affects the function of interacting proteins remains unclear, though the functional consequence is invariably inactivation (27). For some ARF targets, ARF interaction can cause major alterations in metabolic stability, as E2F1 and B23/nucleophosmin are destabilized by proteasome degradation when complexed with ARF (18, 28). Other targets display changes in modification or localization: MDM2 and B23 become sumoylated (42, 51), MDM2 nuclear export is blocked (44), and E2Fs, *c-myc*, and MDM2 are relocalized to the nucleolus (10, 28, 33, 49) upon ARF expression.

Given that the known targets for p53-independent ARF tumor suppression have yet to be precisely assigned to any specific physiologic context related to tumor suppression, we have attempted to identify additional cellular targets of ARF

* Corresponding author. Mailing address: Department of Cancer Biology, University of Massachusetts Medical School, 364 Plantation Street, Worcester, MA 01605. Phone: (508) 856-6423. Fax: (508) 856-1699. E-mail: Steven.Grossman@umassmed.edu.

† These authors contributed equally to this work.

function. By use of a two-hybrid screen, the C-terminal binding protein 2 (CtBP2) transcription regulator was identified as an ARF-binding protein, and ARF interaction caused CtBP degradation by the proteasome. Either ARF expression or CtBP-specific small interfering RNA (siRNA) resulted in apoptosis in p53-null colon cancer cells that was dependent on ARF/CtBP interaction and depletion of cellular CtBP levels.

MATERIALS AND METHODS

Yeast two-hybrid screen. The mouse cDNA encoding full-length ARF was cloned as a NcoI-PstI fragment into pGBKT7, in frame with the GAL4 DNA-binding domain (DBD) (Clontech). A human testis cDNA library in the pACT2 GAL4 activation domain yeast expression vector was obtained from Clontech. For library screening, the *Saccharomyces cerevisiae* reporter strain AH109 (Trp⁻ Leu⁻ His⁻ Ade⁻) was simultaneously transformed with the plasmid pGBKT7/ARF and the cDNA library. The transformed yeast cells were selected by growth on SD dropout medium (Ade⁻ His⁻ Leu⁻ Trp⁻) in the presence of X α -Gal (5-bromo-4-chloro-3-indolyl- β -D-galactopyranoside). The interacting cDNA-derived plasmids were recovered from yeast by reintroduction into *Escherichia coli*, and the identities of putative interacting proteins were determined by sequencing and BLAST search of the NCBI database.

Cell culture and transfections. Mouse embryo fibroblasts (MEFs) (wild type [wt], ARF null, or p53 null) and human U2OS cells were cultured in complete Dulbecco's modified Eagle's medium (DMEM). Human colon cancer (HCT116) cells (ARF silenced) were grown in McCoy's medium. Medium was supplemented with 10% fetal bovine serum-100 U/ml penicillin and incubated in humidified 5% CO₂ at 37°C. Expression plasmids were transfected using Fugene (Roche), and siRNA duplexes were transfected with Oligofectamine (Invitrogen), with an siRNA concentration of 40 nM. siRNA sequences for human CtBP (hCtBP) were as follows: AAACGACUUCACCGUCAAGCA for CtBP1 and AAGCGCCUUGGUCAGUAAUAG for CtBP2.

Plasmid constructions. Full-length CtBP2 was cloned from human lung carcinoma cDNA by use of pCDNA3.1 (Invitrogen), directional TOPO cloning, and specific sense (CACCATGGCCCTTGTGGATA) and antisense (TTGCTCGTTGGGGTGCTC) primers. CtBP2 fragments were inserted in PET 44b (Novagen) at BamHI and HindIII sites. CtBP deletion mutants were constructed in pCDNA3.1 by use of specific PCR primers. The integrity of the plasmids was confirmed by sequencing. pCD-mArf was generated by insertion of a PCR-amplified mArf coding sequence into pCDNA3. Missense and deletion mArf mutants were generated using PCR per the QuikChange protocol (Stratagene). A synthetic mArf gene with arginine codons recoded and optimized for bacterial usage was synthesized from overlapping oligonucleotides and PCR amplified prior to cloning into BamHI/EcoRI sites of pGEX2tk.

Antibodies and Western blotting. Antibodies used were as follows: CtBP1 and CtBP2 (BD Transduction Laboratories), p19^{ARF} (ab80; AbCam), p14^{ARF} (AbCam), glutathione S-transferase (GST) (Z-5; Santa Cruz), V5 tag (Invitrogen), hemagglutinin (HA) (12CA5; Roche), glyceraldehyde-3-phosphate dehydrogenase (GAPDH) (Advanced Immunochemical Inc.), S tag (Novagen), poly(A-ribosyl) polymerase (PARP) (BD Pharmingen), and cleaved caspase 3 (Cell Signaling). Anti-rabbit immunoglobulin G (IgG)-horseradish peroxidase and anti-mouse IgG-horseradish peroxidase conjugates (Amersham) were used with ECL detection (Amersham) for Western blotting.

GST pulldown assays. GST-mArf (codons optimized for *E. coli*) and GST were expressed in BL21. Lysates from U2OS cells transiently transfected with full-length CtBP and mutants were prepared as described previously (5) and incubated with GST or GST-conjugated mArf immobilized on glutathione-Sepharose beads. The beads were washed with wash buffer (10 mM Tris [pH 8.0], 150 mM NaCl, 0.1% Triton X-100, 2 mM MgCl₂, 10 μ M ZnCl₂, 10% glycerol) three times. Protein bound to beads was eluted with 20 mM glutathione in elution buffer (10 mM Tris [pH 8.0], 120 mM NaCl, 0.1% Triton X-100, 10% glycerol), separated by sodium dodecyl sulfate-polyacrylamide gel electrophoresis (SDS-PAGE), and immunoblotted.

S-tag affinity binding assay. CtBP2 mutants expressed in BL21 cells as S-tag fusions in PET vector (Novagen) according to the manufacturer's instructions were incubated with S-protein agarose at 4°C for 1 h. Unbound proteins were washed three times with wash buffer. Lysates from mArf-transfected U2OS cells were incubated with CtBP bound to S-protein agarose at 4°C for 2 h. After the beads were washed three times with wash buffer, the bound protein was released by incubation of the agarose beads in 3 M MgCl₂ for 10 min at room temperature, which was followed by immunoblotting of released proteins for ARF.

Coimmunoprecipitations. Cell lysates (100 μ g of protein) from 1.5 \times 10⁷ cells in lysis buffer (20 mM HEPES, 10 μ M ZnCl₂, 1 mM MgCl₂, 250 mM NaCl, 0.1% Triton X-100, 1 mM dithiothreitol, 1 mM phenylmethylsulfonyl fluoride [PMSF], 10 μ g/ml aprotinin and leupeptin) were incubated at 4°C for 1 h with specific antibody-conjugated Sepharose used for immunoprecipitation. Beads were washed three times in wash buffer (20 mM HEPES, 10 μ M ZnCl₂, 1 mM MgCl₂, 150 mM NaCl, 0.1% Triton X-100, 1 mM PMSF, 10 μ g/ml aprotinin and leupeptin), followed by SDS-PAGE and Western blotting.

UV irradiation. Cells (MEFs and U2OS) were grown to 60% confluence in DMEM with supplements. The medium was removed, and the dishes were exposed to 254-nm UV light (UV-C) at a dose of 0 to 30 J/m² by use of a Stratalinker (Stratagene). The cells were collected 6 h posttreatment, washed with phosphate-buffered saline (PBS), and scraped in lysis buffer supplemented with protease inhibitors. The lysates were then analyzed by Western blotting.

Adenoviral infections. Recombinant hARF (Ad-hARF)- and LacZ (Ad-LacZ)-expressing adenoviruses (52) were the generous gift of T. Kowalik. Cells (10⁶) were plated in 6-well plates 24 h before infection at a confluence of 50%. Cells were washed with PBS once and infected with the Ad-LacZ or Ad-hARF virus in serum-free medium at a multiplicity of infection of 100 at 37°C for 1 h. Virus medium was removed, McCoy's medium was then added, and the cells were incubated for 24 h prior to harvest.

Immunofluorescence. U2OS cells on coverslips were transfected with the indicated mArf and V5-CtBP2 constructs, and 24 h after transfection, cells were fixed and immunostained with anti-CtBP2 and anti-mArf antibodies (AEC40) and anti-rabbit IgG-rhodamine as described previously (28).

[³⁵S]methionine labeling pulse-chase analysis. HCT116 p53^{-/-} cells were infected with Ad-LacZ or Ad-hARF and 24 h later were pulse-labeled for 60 min with [³⁵S]methionine (200 μ Ci/ml; Perkin Elmer) and then chased for various times. The cells were then washed in PBS and lysed with 20 mM HEPES, 10 μ M ZnCl₂, 1 mM MgCl₂, 250 mM NaCl, 0.1% Triton X-100, 1 mM dithiothreitol, 1 mM PMSF, and 10 μ g/ml aprotinin and leupeptin. For immunoprecipitations, cell lysates (100 μ g of protein) were incubated at 4°C for 2 h with CtBP2 antibody-conjugated Sepharose, and beads were washed three times in wash buffer (20 mM HEPES, 10 μ M ZnCl₂, 1 mM MgCl₂, 150 mM NaCl, 0.1% Triton X-100, 1 mM PMSF, 10 μ g/ml aprotinin and leupeptin), followed by SDS-PAGE. Gels were then dried, exposed to Kodak Biomax XAR film, and quantitated by densitometry.

Cell cycle and apoptosis analysis. For cell cycle analysis of cells expressing mArf, 10⁶ 3T3-D1 cells (32) were transfected with 5 μ g of pCD-mArf plasmid plus 0.5 μ g plasmid encoding membrane-targeted green fluorescent protein (GFP). Forty-eight hours after transfection, cells were trypsinized, washed once in cold PBS, fixed in 5 ml cold methanol (-20°C) for 30 min, centrifuged, and resuspended in 0.5 ml PBS containing RNase A (50 μ g/ml) and propidium iodide (100 μ g/ml). The cells were then subjected to flow cytometric analysis with gating for GFP. For each sample, 5,000 GFP-positive cells were collected and cell cycle distribution was analyzed according to relative DNA content. For viability analysis, cells were trypsinized and mixed 1:1 with trypan blue solution (0.8 mM in PBS) and counted with a hemacytometer. An annexin V-PE apoptosis detection kit (where PE is phycoerythrin) from BD Pharmingen was used according to the manufacturer's instructions to identify cells undergoing apoptosis. A Caspa Tag Caspase-3/7 in situ assay kit (Chemicon International) was used for in situ detection of activated caspases 3 and 7 by fluorescence-activated cell sorter (FACS) analysis.

RESULTS

Two-hybrid screen for ARF-interacting proteins. To identify ARF-interacting proteins that might explain the p53-independent effects of ARF, a two-hybrid screen using mArf as bait was performed against prey cDNAs derived from a human testis cDNA library. A C-terminal fragment (residues 224 to 445) of hCtBP2 was identified in 4 of 12 colonies. CtBP proteins are transcriptional corepressors with a protein interaction domain near their N termini that recognizes a PLDLS sequence, an NADH-binding central dehydrogenase regulatory domain, and a C-terminal PDZ-binding domain (Fig. 1A) (9). The N-terminal PLDLS interaction domain was excluded from the portion recovered in the two-hybrid screen. On rescreen, by use of a GAL4 upstream activation sequence-LacZ reporter

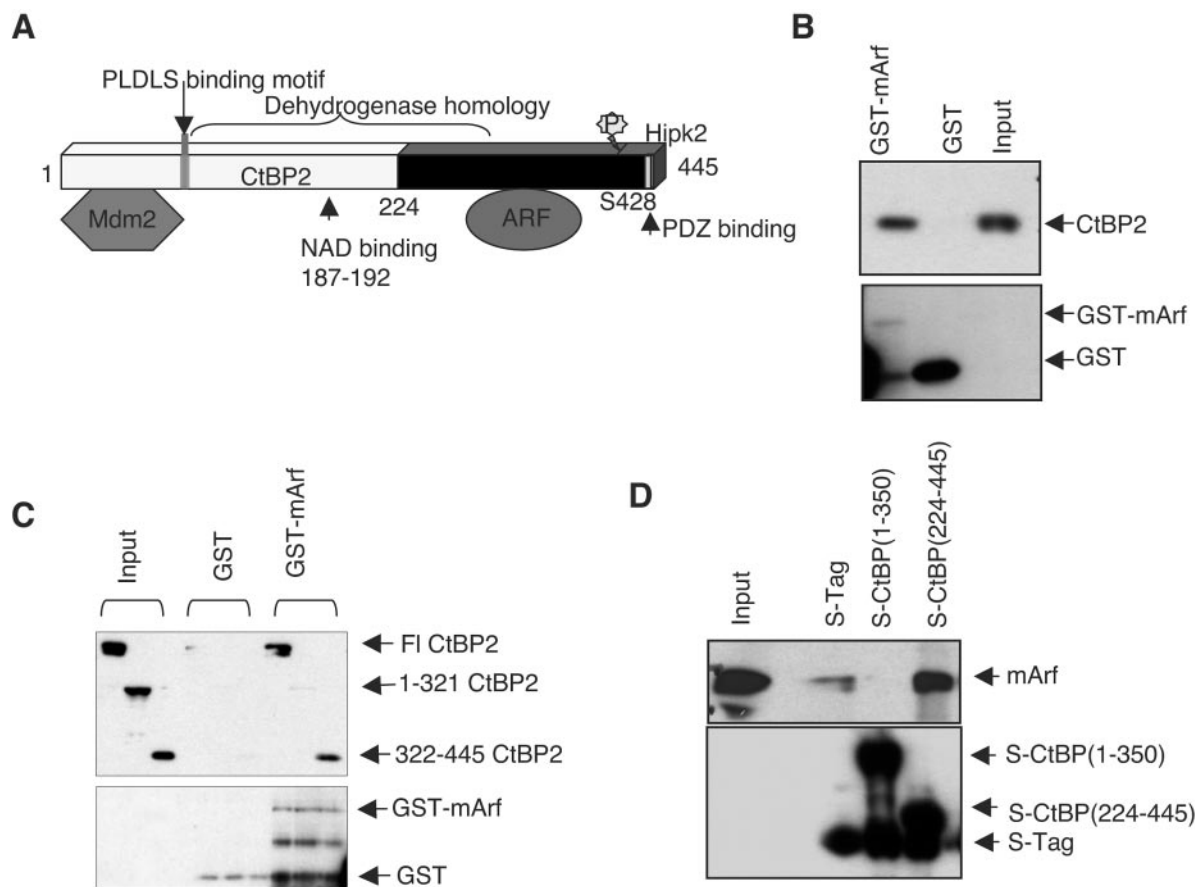


FIG. 1. ARF interacts with CtBP. (A) Schematic representation of CtBP functional domains and the ARF binding region at the C terminus, as identified by a two-hybrid screen. The HIPK2 phosphorylation (P) site (S428) is noted. (B) CtBP interacts with ARF *in vitro*. GST or GST-mArf fusion proteins were conjugated to glutathione-agarose beads and incubated with U2OS cell lysates. Bound, endogenous CtBP2 was assayed by Western blotting. Input lane shows 10% of the cell lysate. GST and GST-mArf migration positions are indicated by arrows. (C) The CtBP C terminus interacts with ARF. V5-tagged full-length (FL), N-terminal (1–321), and C-terminal (322–445) hCtBP2 proteins were expressed in U2OS cells. Binding of V5-hCtBP2 proteins to GST versus GST-mArf was assayed by immunoblotting of GST pulldowns. Arrows indicate the migration positions of the wild type and deletion mutants of V5-hCtBP2 as well as GST-mArf. (D) The CtBP C terminus interacts with ARF. S-tagged C-terminal (224–440) or N-terminal (1–350) hCtBP2 fusion proteins or unfused S-tag protein were expressed in *E. coli*, purified with S-protein agarose, and incubated with a lysate of mArf-expressing U2OS cells. Bound mArf and the presence of S-tag fusion proteins were determined by immunoblotting.

and an α -galactosidase assay, hCtBP2 was found to interact strongly with the GAL4 DBD fusion to mArf but not with the GAL4 DBD alone, indicating that the interaction occurred specifically through the ARF portion of the GAL4 DBD-mArf fusion protein.

ARF and CtBP interact *in vitro*. To further characterize the putative ARF/CtBP interaction, purified GST or GST-mArf fusion proteins were incubated with U2OS cell lysates (Fig. 1B). GST-mArf, but not GST, was able to specifically recognize the endogenous 48-kDa hCtBP2 protein from U2OS cell lysates, suggesting that these proteins can specifically interact both *in yeast* and *in vitro*.

In an effort to map the binding of mArf to hCtBP2, V5-tagged full-length (V5-hCtBP2-FL), N-terminal (residues 1 to 321) [V5-hCtBP2(1–321)], and C-terminal (residues 322 to 445) [V5-hCtBP2(322–445)] constructs of hCtBP2 were transiently expressed in U2OS cells, followed by analysis for binding of the V5-hCtBP2 proteins to purified GST versus GST-mArf. Consistent with the yeast two-hybrid data, V5-hCtBP2-FL and V5-

hCtBP2(322–445), but not V5-hCtBP2(1–321), bound specifically to GST-mArf (Fig. 1C).

Likewise, mArf expressed in U2OS cells bound to S-tagged C-terminal (residues 224 to 445) [S-CtBP2(224–445)] but not S-tagged N-terminal (residues 1 to 350) [S-CtBP2(1–350)] hCtBP2 fusion proteins produced in *E. coli* (Fig. 1D). Moreover, ARF is highly basic and thus prone to nonspecific protein-protein interactions (50). The lack of detectable mArf binding to V5-hCtBP2(1–321) or S-CtBP2(1–350), which were produced in different systems and tested against bacterially or eukaryotically synthesized mArf, strongly suggests that ARF interaction with the CtBP C terminus is specific.

ARF interacts with CtBP *in vivo*. To determine whether ARF/CtBP interaction could be observed in cells and whether it is regulated by cellular stress, such as UV exposure, U2OS cells were transfected with V5-hCtBP2 and full-length mArf expression vectors, followed by UV or mock irradiation. Transfected cell lysates were then immunoprecipitated with anti-V5, anti-ARF, or control anti-ras antibody, followed by immuno-

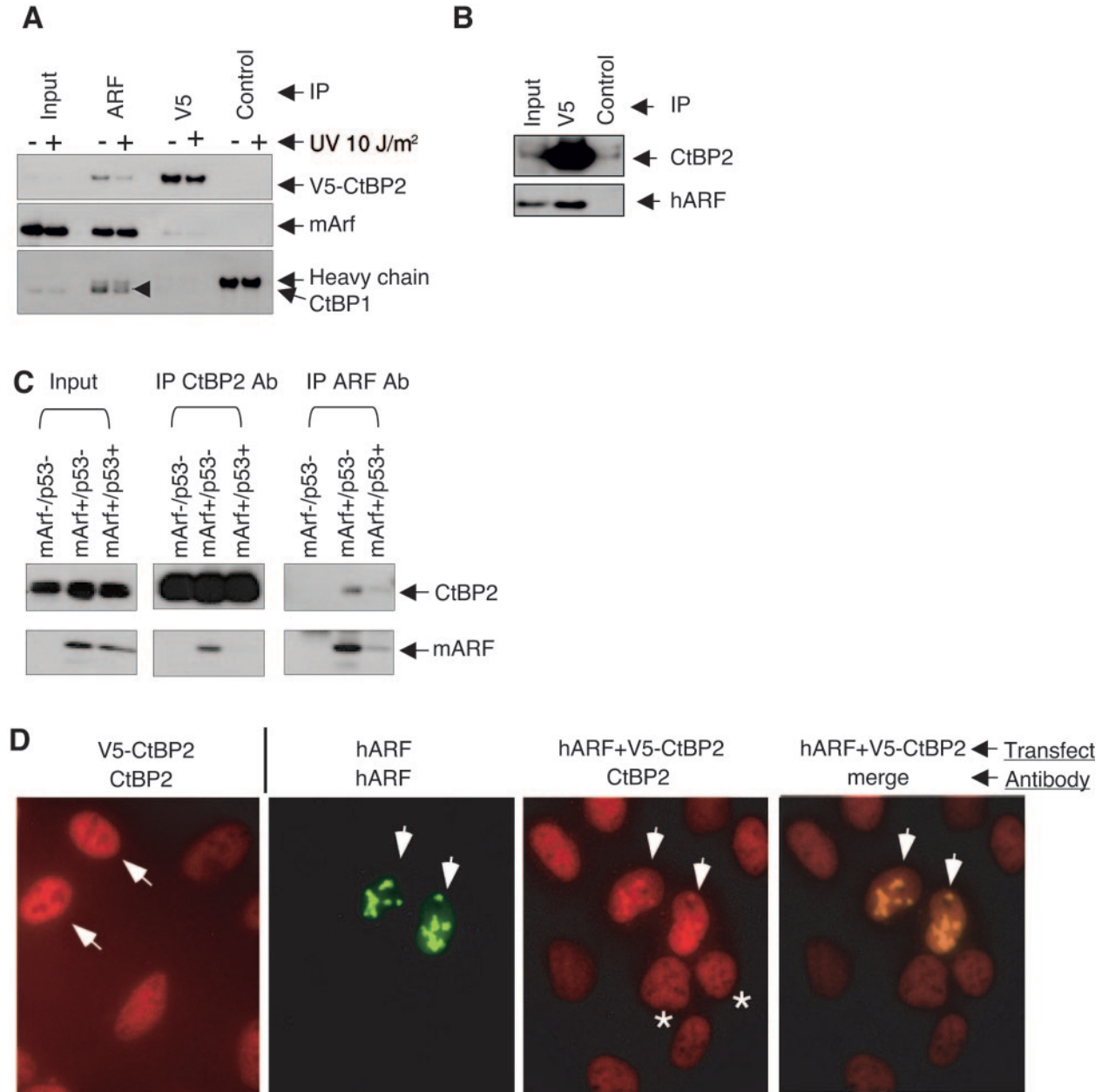


FIG. 2. In vivo ARF interaction with CtBP. (A) Exogenous CtBP interacts with exogenous ARF in transfected cells. U2OS cells were transfected with V5-hCtBP2 and mArf expression plasmids and UV or mock irradiated (10 J/m²) 24 h after transfection. Six hours after UV exposure, cell lysates were immunoprecipitated with anti-ras (control), anti-ARF, or anti-V5 antibody, followed by Western blot analysis with anti-V5, anti-CtBP1, or anti-ARF antibody. Input lane depicts 10% of the transfected cell lysate. (B) hARF interacts with CtBP. U2OS cells were transfected with V5-hCtBP2 and myc-hARF expression plasmids. Immunoprecipitation was performed with V5 or control antibody (Ab), followed by immunoblotting for hARF and V5. (C) (Middle and right panels) In vivo coimmunoprecipitation of mArf and mCtBP2 from lysates of wt, p53-null, or p53/mArf-null MEFs. Immunocomplexes were analyzed for the presence of endogenous ARF and mCtBP2 by Western blotting. (Left panel) 10% of input protein lysates. (D) CtBP2 and hARF colocalize. U2OS cells were transfected with hARF, V5-CtBP2, or both expression plasmids. Twenty-four hours after transfection, cells were immunostained with rabbit anti-hARF and mouse anti-hCtBP2 antibodies, followed by detection with fluorescein isothiocyanate-labeled (anti-rabbit) or rhodamine-labeled (anti-mouse) secondary antibody. Arrows indicate cells that were transfected, as noted by a CtBP2 level increased above that seen with adjacent untransfected cells. The merged image highlights relocation of CtBP2 to nuclear bodies consistent with nucleoli, where hARF is found. Asterisks indicate untransfected cells.

blotting with V5 and ARF antibodies. The negative control, anti-ras antibody immunoprecipitate (IP), was clear of ARF, V5-hCtBP2, and hCtBP1 (Fig. 2A). ARF was evident in the anti-V5 IPs, and V5-hCtBP2 was detected in the anti-ARF IPs (Fig. 2A, -UV), consistent with a specific ARF/CtBP interaction *in vivo*, though UV irradiation had no impact on binding (Fig. 2A, +UV).

To investigate whether ARF interacts with the highly similar CtBP1 protein (23), the V5 and ARF IPs were also probed for the presence of hCtBP1. Cellular hCtBP1 was detected in the ARF IP but not in the V5 IP, suggesting that it also interacts with ARF and that its presence in the ARF IP was not due to oligomerization with exogenous V5-hCtBP2 protein (Fig. 2A).

Similarly to mArf, exogenously expressed myc-tagged human ARF protein (myc-hARF) was present in an anti-V5 IP, but not a control IP, of a cell lysate derived from U2OS cells cotransfected with myc-hARF and V5-hCtBP2 expression plasmids (Fig. 2B), suggesting that both hARF and mArf interact with CtBP.

To confirm that ARF and CtBP form an endogenous physiologic complex in mammalian cells, lysates from MEFs that were wt, null for p53, or null for both p53 and ARF were immunoprecipitated with either anti-CtBP2 or anti-ARF antibody. ARF was more abundant in p53-null MEFs, as expected, due to loss of p53 negative feedback on ARF expression (16) (Fig. 2C). ARF coimmunoprecipitated with CtBP2, and vice versa, when protein extracts were prepared from wild-type and p53-null MEFs (Fig. 2C, second and third lanes of each panel). The higher efficiency of the coimmunoprecipitate in p53-null cell lysates reflected, in part, the greater baseline abundance of ARF. A further effect of p53 loss on the avidity of mArf/CtBP2 interaction is also possible, as the increase in the amount of bound mArf in the CtBP IP between wt and p53-null MEFs was substantially greater than the observed difference in expression level of mArf between the two cell types. Cell lysates from ARF-null cells were negative for ARF/CtBP2 coimmunoprecipitation, demonstrating that detection of CtBP2 in the ARF IP required the specific presence of ARF protein and that the putative ARF immunoblot signal in the CtBP IPs was also dependent on the presence of ARF in the cell lysates (Fig. 2C, first lane of each panel).

ARF relocates CtBP to the nucleolus. To further investigate the physiologic significance of CtBP and ARF biochemical interaction, HCT116 p53^{-/-} cells were transfected with V5-CtBP2 and vector or hARF expression plasmids, followed by staining with anti-hARF and CtBP2 antibodies (Fig. 2D). CtBP2 was exclusively nucleoplasmic in transfected or untransfected cells and was excluded from unstained nuclear structures consistent with nucleoli (Fig. 2D, first panel). Conversely, hARF displayed its typical nucleolar staining pattern (Fig. 2D, second panel) (26, 50, 55), and its coexpression with CtBP2 resulted in nearly quantitative relocalization of CtBP2 into the same subnuclear structures as hARF (Fig. 2D, third and fourth panels). Consistent with the hARF dependence of CtBP2 relocalization, cells within the same culture that did not express exogenous CtBP2 and hARF retained the normal nucleoplasmic and nucleolar-excluded localization of CtBP2 (Fig. 2D, third panel).

A conserved hydrophobic domain of ARF recognizes CtBP. In order to identify the region of ARF required for CtBP

interaction, lysates of U2OS cells transfected with wild-type or mutant mArf expression plasmids were immunoprecipitated with hCtBP2 antibodies, followed by analysis of the IPs by anti-ARF immunoblotting. mArf mutants defective for MDM2 binding (deletion of residues 8 to 32 [Δ 8-32]) or nucleolar localization (Δ 26-37) or targeting an uncharacterized but conserved (with human ARF) region of exon 1 β (Δ 32-51, Δ 46-51, and L46D) were included in this analysis (Fig. 3A). Whereas wt, Δ 8-32, and Δ 26-37 ARF proteins all coimmunoprecipitated with CtBP (Fig. 3A, lanes 1 to 3), the L46D, Δ 32-51, and Δ 46-51 ARF proteins did not (Fig. 3A, lanes 4 to 6). Thus, mArf residues between 37 and 51 or, at a minimum, 46 and 51 were required for hCtBP2 interaction, whereas the MDM2 interaction and nucleolar localization domains at the ARF N terminus (residues 2 to 37) (3, 27, 49) were not.

As might be expected based on prior mapping of mArf functional domains (49), loss of residues 46 to 53 or an L46D mutation had little or no effect, whereas deletion of residues 8 to 32 of mArf rendered it unable to interact with MDM2, localize to the nucleolus, block MDM2-dependent p53 degradation, or induce G₁ cell cycle arrest in mouse fibroblasts (Fig. 3B to E). Thus, mArf-CtBP interaction does not require simultaneous mArf-MDM2 interaction, and mutations in the CtBP-binding region of mArf do not grossly disrupt its ability to interact with and inhibit MDM2.

ARF induces proteasome-dependent CtBP depletion. CtBP is reportedly degraded by the proteasome after UV exposure, leading to apoptosis (54). Notably, the human cancer cell lines with which CtBP degradation was observed after UV exposure invariably expressed ARF (54), suggesting that a potential function of ARF/CtBP interaction is to induce CtBP degradation.

To more precisely define the necessity of mArf and/or p53 for CtBP degradation after UV exposure, a panel of MEFs null for either or both p53 and mArf were screened for UV-induced mouse CtBP2 (mCtBP2) degradation (Fig. 4A to D). Cells in which mArf expression was absent (mArf^{-/-} and mArf p53^{-/-} MEFs) did not display changes in their mCtBP2 levels after exposure to 5 to 30 J/m² of UV-C (Fig. 4A and B), whereas cells retaining mArf expression (wt and p53^{-/-} MEFs) showed decreased (average of 30 to 40% reduction) mCtBP2 levels (Fig. 4C and D). mCtBP2 degradation was optimal after exposure to doses of UV-C in the range of 5 to 20 J/m², but higher doses of UV did not affect mCtBP2 level, perhaps reflecting the differential activation of signaling pathways that occurs at higher UV doses (20) or, more simply, overwhelming cellular damage. Consistent with previous data obtained from human cells, proteasome inhibition blocked UV-induced degradation of mCtBP2 (Fig. 4E) (54). Thus, mArf expression in mouse fibroblasts correlates with UV-induced proteasome degradation of mCtBP2.

UV-induced CtBP2 degradation requires mArf/CtBP2 interaction. To determine if mArf/CtBP interaction was linked specifically to UV-induced CtBP degradation, mArf wt or mutant alleles were introduced into hARF-negative U2OS cells (Fig. 5A and B). Expression of mArf sensitized U2OS cells to UV-induced loss of hCtBP2 (optimal effect at 10 J/m²) (Fig. 5A). Wild-type or mutant mArf alleles were then coexpressed with GFP in U2OS cells, and transfected cells were isolated by sorting for GFP. All mArf alleles were expressed at comparable levels (Fig. 5B, top panel). Consistent with a role of ARF

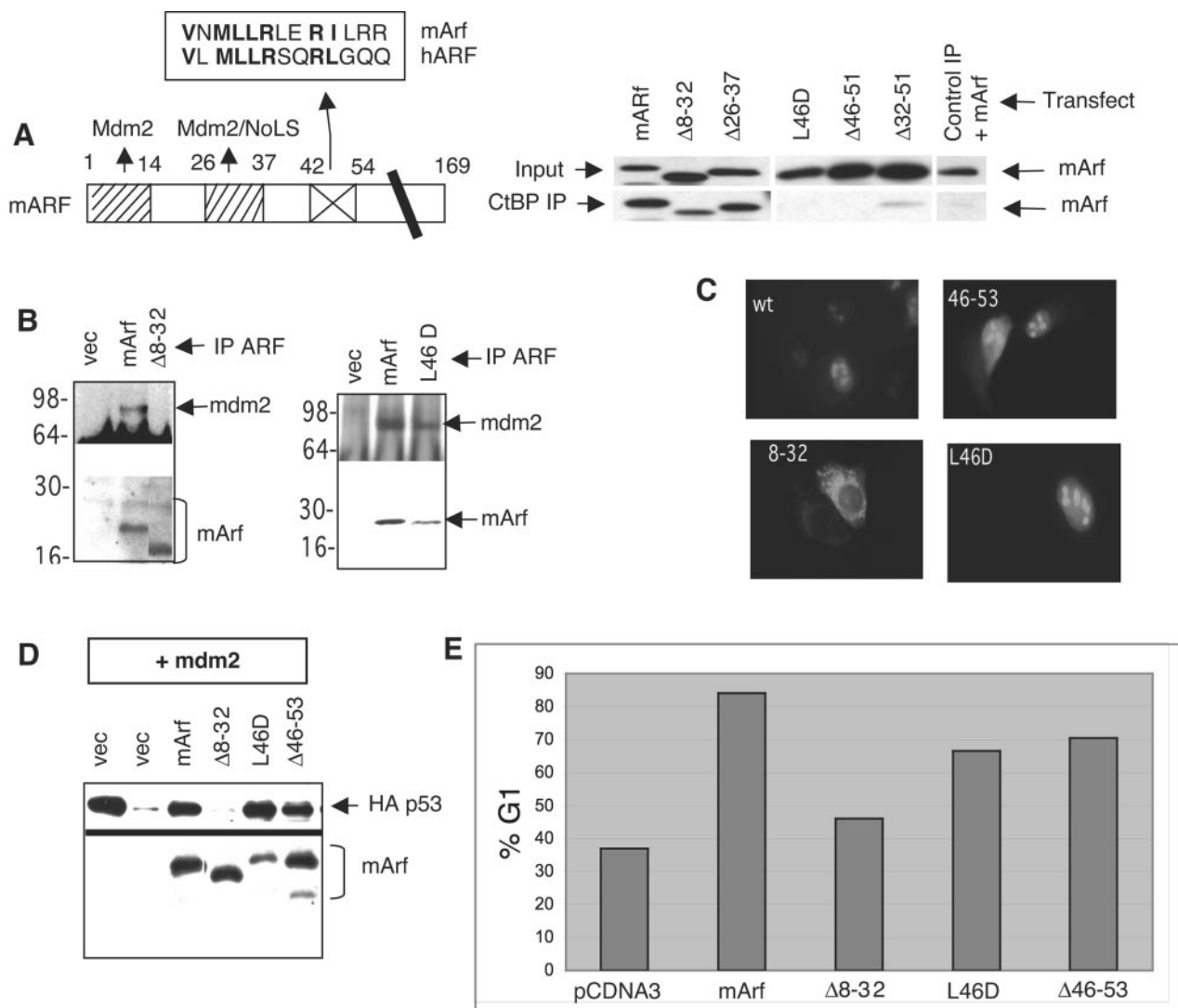


FIG. 3. The CtBP and MDM2 interaction domains of ARF are distinct. (A) (Left) ARF schematic showing MDM2 binding and nucleolar localization (NoLS) domains and a third conserved ARF domain of unknown function with human/mouse ARF amino acid sequence alignment (top). Conserved residues within this domain are set in boldface type. (Right) Lysates of U2OS cells transfected with wt or mutant mArf expression plasmids were immunoprecipitated with CtBP2 antibody, followed by analysis of the IPs by anti-ARF immunoblotting. Control IP was performed with anti-ras antibody using lysates of cells transfected with full-length mArf. (B) Mutations within the CtBP-binding region of mArf do not disrupt MDM2 interaction. U2OS cells were transfected with the indicated mArf expression plasmids and lysates immunoprecipitated with anti-ARF antibody (AEC40), followed by MDM2 and ARF immunoblotting. Numbers at left are molecular size markers (in kDa). vec, vector. (C) Mutations within the CtBP-binding region of mArf do not disrupt nucleolar localization. U2OS cells were transfected with the indicated mArf expression plasmids, and transfected cells were immunostained with ARF antibody (AEC40). All mArf alleles, except Δ8-32, which lacks the NoLS (amino acids 26 to 37), properly localize to nuclear bodies consistent with the appearance of nucleoli. (D) mArf mutations within the CtBP-binding region do not disrupt inhibition of MDM2-mediated p53 degradation. U2OS cells were transfected with HA-p53, MDM2, and the indicated mArf expression plasmids, followed by immunoblotting of transfected cell lysates with HA and ARF antibodies. (E) Mutations within the CtBP-binding region of mArf do not grossly disrupt induction of G₁ arrest. Mouse 3T3-D1 cells (p53 wt) were transfected with the indicated mArf expression plasmids and GFP, and cell cycle profiles of GFP-gated cells were analyzed by propidium iodide staining and FACS analysis 48 h after transfection. A representative experiment is shown; the experiment was repeated three times with similar results.

interaction in directing CtBP degradation, expression of mArf mutants defective for hCtBP2 interaction (L46D and Δ46-51) did not induce hCtBP2 loss in UV-treated cells, whereas wt mArf or mArf(Δ8-32), which is defective for MDM2 interaction and nucleolar localization, were fully competent for directing hCtBP2 degradation after UV exposure (Fig. 5B, middle panel). Thus, the ability of mArf to form a biochemical complex with CtBP, but not its potential for MDM2 interaction

or nucleolar localization, correlated with its ability to direct CtBP degradation.

Though ARF/CtBP2 interaction was required for UV-induced CtBP2 degradation, it did not appear that the mechanism of the UV effect involved specific regulation of ARF/CtBP2 interaction. As noted in Fig. 2A, UV irradiation had no influence on the avidity of ARF/CtBP2 interaction. Additionally, CtBP2 mutated at a putative UV-regulated HIPK2 phos-

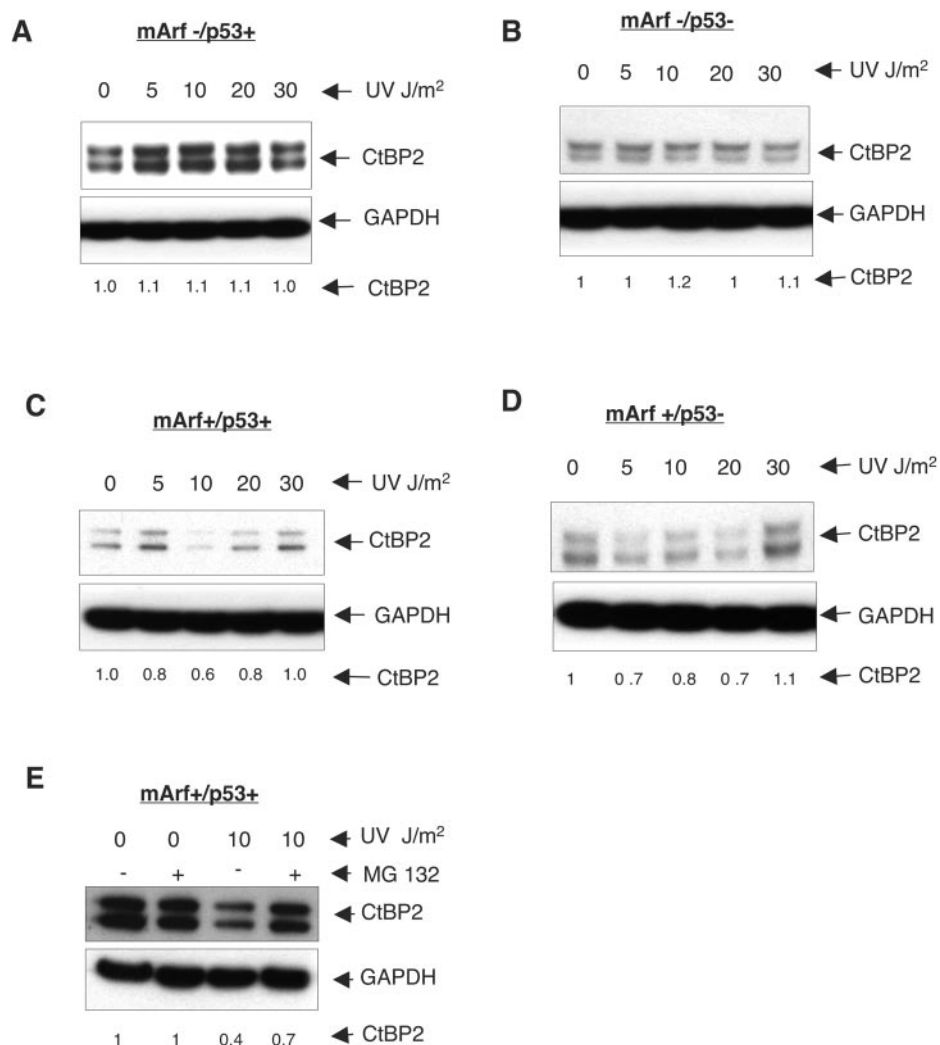


FIG. 4. UV induced CtBP degradation by the proteasome correlates with cellular ARF status. (A to D) MEFs of various mArf and p53 statuses were exposed to increasing doses of UV-C (0 to 30 J/m²). Levels of endogenous mCtBP2 6 h after UV treatment were determined by Western blotting. CtBP2 levels were quantitated by densitometry and normalized to a GAPDH loading control. (E) mCtBP2 is degraded by the proteasome in response to UV. MEFs (mArf⁺ p53⁺) were incubated with or without proteasome inhibitor (MG132) for 24 h after mock or UV (10 J/m²) treatment. Cell lysates were analyzed for changes in CtBP2 level by Western blotting, followed by densitometry normalized to a GAPDH loading control. Experiments were repeated a minimum of three times with similar results, and data from representative experiments are shown in panels A to E. Numbers below blots represent GAPDH-normalized relative levels of CtBP2.

phorylation site (based on CtBP1 homology; S428A) (54) bound to ARF similarly to wt CtBP2 in the presence or absence of UV (data not shown).

Human ARF causes CtBP2 depletion in the absence of stress. To confirm that human and mouse ARF induced similar effects on CtBP metabolism, hARF was introduced into HCT116 colon cancer cells that were wild type or null for p53 (6) by use of a recombinant adenovirus (52). Surprisingly, hARF expression alone, without addition of UV or other types of stress, resulted in a profound loss of hCtBP2 that was not seen with cells infected with a LacZ-expressing virus and that occurred irrespective of p53 status (Fig. 5C). hCtBP1 was similarly affected by acute expression of hARF in HCT116 p53^{-/-} cells (Fig. 5D).

The loss of CtBP after Ad-hARF infection was not influenced by expression of adenoviral genes or signals generated by viral

entry, as hARF protein synthesized from a transfected plasmid similarly caused CtBP depletion (Fig. 5E, second lane). However, the link between ARF/CtBP2 interaction and CtBP2 depletion was demonstrated by the inability of a hARF protein mutated at the site homologous to mArf L46 [hARF(L50D)] to likewise induce CtBP loss (Fig. 5E, third lane).

ARF destabilizes CtBP2 without affecting ubiquitination status. To determine if the effect of exogenous ARF on hCtBP2 was posttranscriptional, a semiquantitative reverse transcriptase PCR analysis was performed with CtBP2-specific primers on mRNA purified from Ad-LacZ- and Ad-hARF-treated HCT116 p53^{-/-} cells (Fig. 5F). Despite the decreased abundance of CtBP2 protein in hARF-expressing cells, no significant change in CtBP2 mRNA abundance was seen, suggesting that the effect of hARF on CtBP2 protein level occurred through a posttranscriptional mechanism.

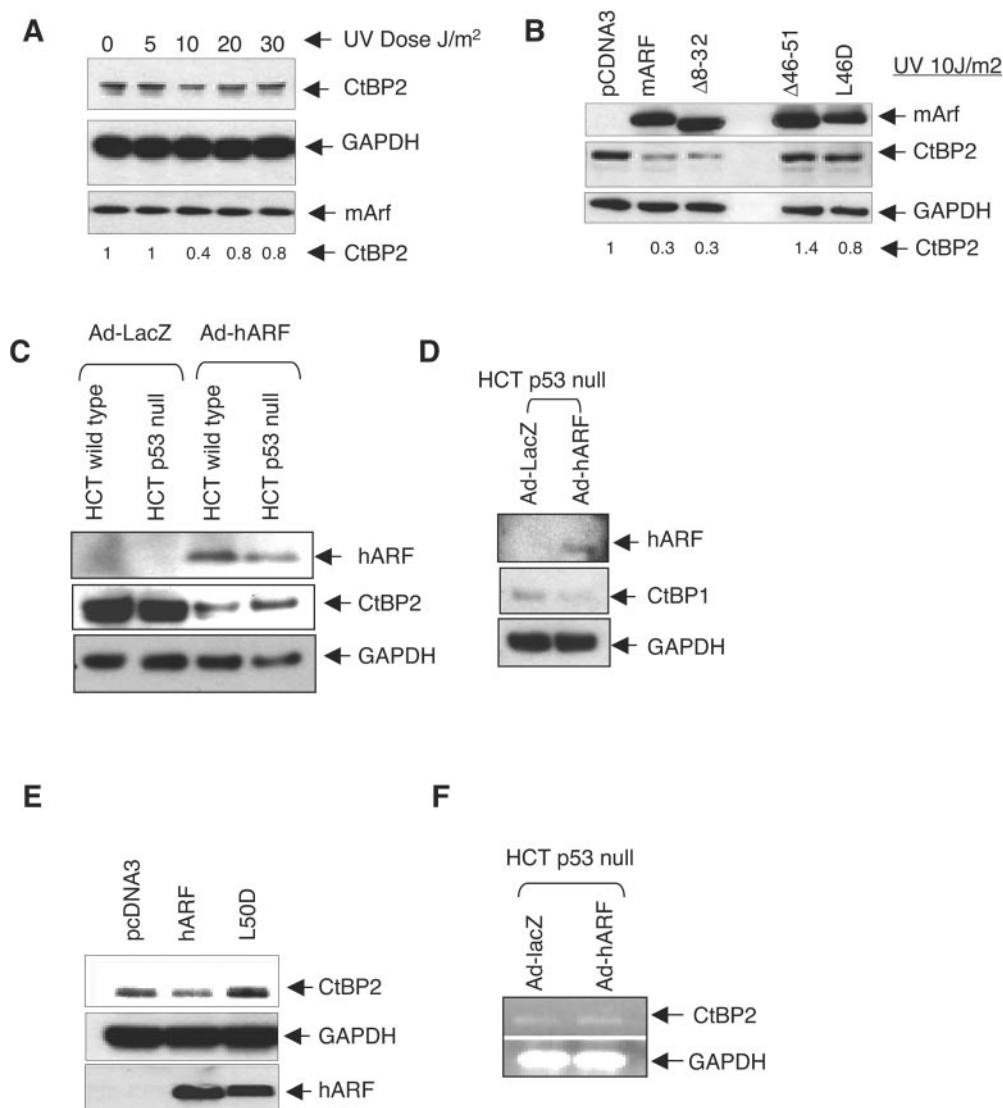


FIG. 5. ARF causes CtBP degradation. (A) U2OS (hARF-null) cells were transfected with vector control or full-length mArf expression plasmids, followed by mock or UV treatment (UV-C at 0 to 30 J/m²), and CtBP2, hARF, and GAPDH levels were determined by immunoblotting 6 h after UV treatment. CtBP2 levels were quantitated by densitometry and normalized to GAPDH. (B) Degradation of endogenous CtBP by mArf mutants. Indicated ARF expression plasmids were transfected into HCT116 p53^{-/-} cells along with pCD-GFP and treated with UV-C at 10 J/m² 24 h after transfection. Transfected cells were sorted for GFP 6 h after UV treatment, lysed, and analyzed by immunoblotting for CtBP2. CtBP2 levels were quantitated by densitometry and normalized to GAPDH. (C) hARF causes CtBP loss without stress. Lysates of HCT116 and HCT116 p53^{-/-} cells obtained 24 h postinfection with Ad-LacZ or Ad-hARF were immunoblotted with ARF, CtBP2, or GAPDH specific antibody. (D) ARF causes CtBP1 loss. Lysates of HCT116 p53^{-/-} cells infected with Ad-LacZ or Ad-hARF, as described for panel C, were assayed for ARF, CtBP1, and GAPDH expression by immunoblotting. (E) hARF-induced CtBP2 degradation requires an intact CtBP recognition domain. HCT116 p53^{-/-} cells were transfected with vector, hARF, or hARF(L50D) mutant expression plasmids, followed by sorting for GFP 24 h after transfection. Cell lysates of GFP-expressing cells were analyzed by hCtBP2, GAPDH, and hARF immunoblotting. (F) hARF does not affect hCtBP2 mRNA level. Semiquantitative (18 cycles) reverse transcriptase PCR of mRNA prepared from HCT116 p53^{-/-} cells infected with Ad-LacZ or Ad-hARF was carried out using CtBP2 and GAPDH specific primers. Numbers below blots in panels A and B represent GAPDH-normalized relative levels of CtBP2.

To determine if metabolic instability of CtBP2 upon hARF expression could account for its loss of abundance, a pulse-chase analysis of the CtBP2 half-life was performed using CtBP2 immunoprecipitated from [³⁵S]methionine pulse-labeled HCT116 p53^{-/-} cells expressing LacZ or hARF. As seen in Fig. 6A, the half-life of CtBP2 in LacZ-expressing cells was indeterminately long, whereas in ARF-expressing cells, the CtBP2 half-life was decreased to ~4 h. Thus, hARF-induced

CtBP2 depletion in cells correlates with metabolic destabilization of CtBP2.

Proteasome-mediated destabilization of CtBP2 may have resulted from increased ubiquitination (53). The potential for ARF to modulate CtBP2 ubiquitination was assessed by coexpressing CtBP2 and HA-ubiquitin in HCT116 p53^{-/-} cells, followed by infection with Ad-LacZ or Ad-hARF. Prior to lysis, cells were treated with MG132 proteasome inhibitor to

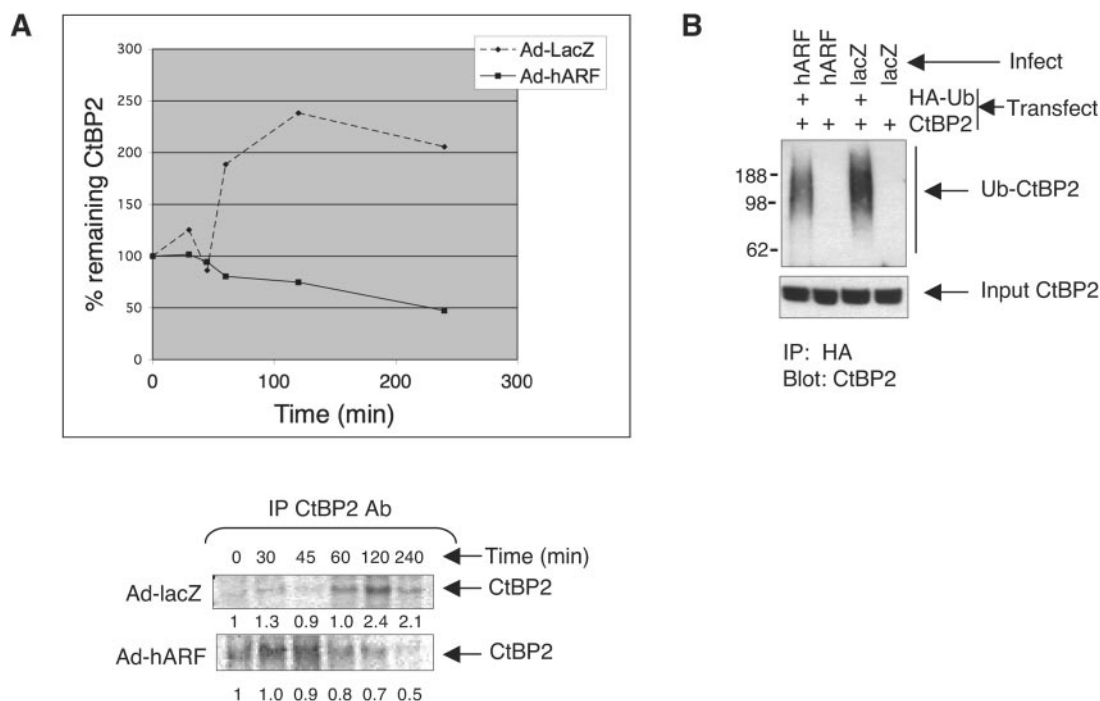


FIG. 6. ARF destabilizes CtBP2 without altering its ubiquitination. (A) hARF causes hCtBP2 destabilization. Twenty-four hours after Ad-LacZ or Ad-hARF infection, HCT116 p53^{-/-} cells were pulse-labeled with [³⁵S]methionine, followed by chase in unlabeled DMEM. At indicated times during the chase, aliquots of cells were lysed and run directly on SDS-PAGE (not shown) or immunoprecipitated with anti-hCtBP2, followed by SDS-PAGE and autoradiography. Relative hCtBP2 levels (numbers below autoradiogram) were quantitated by densitometry and normalized against [³⁵S]methionine incorporation as assayed for each sample by SDS-PAGE and autoradiography of total [³⁵S]methionine-labeled proteins. (B) Effect of hARF on CtBP2 ubiquitination. HCT116 p53^{-/-} cells were transfected with CtBP2 and HA-ubiquitin (HA-Ub) expression plasmids, and 16 h later, transfected cells were infected with Ad-LacZ or Ad-hARF. Twenty-four hours after infection, lysates were immunoprecipitated with anti-HA agarose, followed by CtBP2 immunoblotting. Ub-CtBP2 indicates the migration position of ubiquitinated CtBP2 species. Numbers at left are molecular size markers (in kDa).

protect ubiquitin chains from degradation and to increase the sensitivity of ubiquitin-conjugate detection. Transfected cell lysates were immunoprecipitated with HA antibody, and the IPs were immunoblotted for CtBP2. As seen in Fig. 6B, no change, or a possible decrease in the abundance of ubiquitinated CtBP2, was noted upon ARF expression. Thus, destabilization of CtBP2 by hARF is not accompanied by an appreciable increase in CtBP2 ubiquitination, though CtBP2 is ubiquitinated even in resting HCT116 p53^{-/-} cells.

CtBP depletion by ARF or siRNA is sufficient to trigger p53-independent apoptosis. To determine if CtBP depletion, as induced by ARF, could be linked to a physiologic tumor suppression function, the effect of direct depletion of CtBP2 using siRNA was tested in cells that were wild type or null for p53. Previous reports have indicated that, unlike mArf, hARF can induce apoptosis in the absence of p53, though by an undefined mechanism (17). To confirm that hARF induces apoptosis in the absence of p53, HCT116 cells that were wt or null for p53 were infected with Ad-hARF or Ad-LacZ; both cell types were assayed for activation of the apoptotic program via flow cytometric assay for cleaved caspase 3 (Fig. 7A), and p53-null cells were also assayed for viability by use of trypan blue exclusion (Fig. 7C). After Ad-hARF but not Ad-LacZ infection, both cell types exhibited significant activation of caspase 3 (20 to 23% of counted cells) (Fig. 7A), while p53-null cells exhibited a concomitant loss of viability (Fig. 7C).

HCT116 cells (p53 wt or null) were then exposed to CtBP1, CtBP2, or control siRNA and assayed for cleavage of caspase 3, presence of the caspase-cleaved fragment of PARP, and viability (p53-null cells only) (Fig. 7B and C). CtBP1 or CtBP2 siRNA treatment caused a substantial loss of viability in HCT116 p53^{-/-} cells (Fig. 7C) compared to control siRNA treatment, suggesting that loss of CtBP expression is lethal. Consistent with an apoptotic mechanism for cell death in CtBP siRNA-treated cells, cleaved forms of both caspase 3 and PARP were observed with both wild-type and p53-null HCT116 cells treated with hCtBP1 or hCtBP2 siRNA but not control siRNA (Fig. 7B).

Surprisingly, hCtBP1 levels were consistently decreased after hCtBP2 siRNA treatment, but not vice versa (Fig. 7B). This may be due to a cross-reaction of hCtBP2 siRNA with hCtBP1 mRNA or direct effects of hCtBP2 on the hCtBP1 promoter and may account for the more robust effects of hCtBP2 siRNA on induction of caspase activity (Fig. 7B). Thus, a decrease in CtBP1 or CtBP2 levels, either by siRNA or after ARF expression, lowers the cellular apoptotic threshold, resulting in spontaneous p53-independent apoptosis.

ARF-induced p53-independent apoptosis requires CtBP interaction and CtBP depletion. To correlate ARF-induced apoptosis with the ability of ARF to degrade and deplete cellular CtBP, CtBP2 was replaced in ARF-expressing cells with exogenous protein synthesized from an expression vector. HCT116

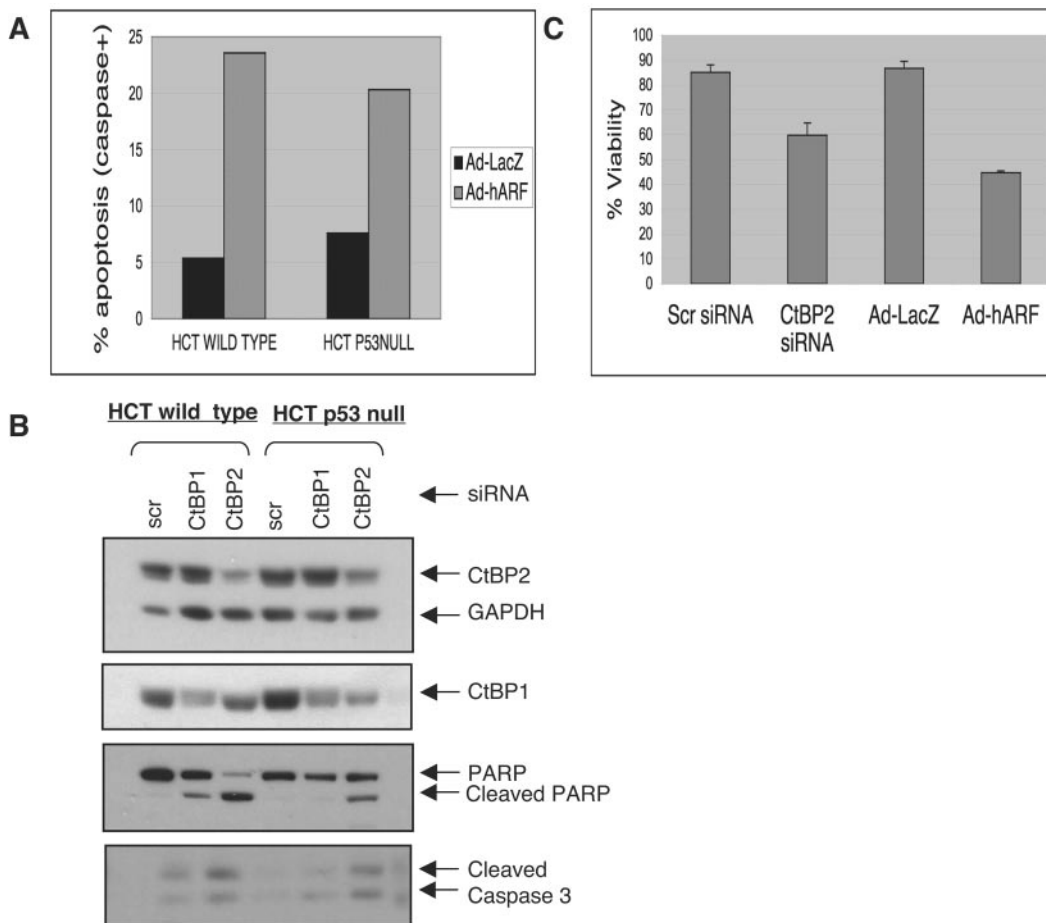


FIG. 7. ARF expression or CtBP depletion causes p53-independent apoptosis. (A) ARF induces p53-independent apoptosis. Twenty-four hours after infection with Ad-LacZ or Ad-hARF, HCT116 wt or p53-null cells were labeled with fluorescent caspase 3/7 substrate and propidium iodide and assayed by FACS analysis. The percentages of live cells with active caspase 3 in each sample were plotted. A representative experiment is shown, and similar results were seen with four separate repetitions. (B) CtBP depletion induces apoptosis. HCT116 wt or p53-null cells were treated with siRNA duplexes complementary to either hCtBP2 or hCtBP1. Specific depletion of hCtBP1 or hCtBP2 and identification of PARP and caspase 3 cleavage products were determined by immunoblotting. (C) hARF expression or CtBP siRNA reduces cell viability in the absence of p53. Percent viable cells, as determined by trypan blue exclusion (mean from three independent experiments), was plotted for CtBP knockdown compared to control siRNA treatment and for Ad-hARF infection compared to Ad-LacZ infection in HCT116 p53^{-/-} cells. Error bars indicate 1 standard deviation. scr, scrambled.

p53^{-/-} cells were transfected with control vector or V5-CtBP2 expression plasmid, followed by infection with Ad-LacZ or Ad-hARF. Twenty-four hours after infection, cells were assayed for apoptosis induction by an annexin V flow cytometry assay (Fig. 8A, left panel). Expression of ARF and CtBP2 was confirmed by immunoblotting (Fig. 8A, right panel). Expression of CtBP in LacZ-expressing cells caused no significant change in annexin V positivity (Fig. 8A, left panel). ARF was potently apoptogenic, with a tripling in the fraction of apoptotic cells (from 14% to 42%), whereas exogenous CtBP expression completely rescued cells from ARF-induced apoptosis, with a rate of annexin V positivity comparable to that seen in control vector-transfected, LacZ-expressing cells (10%) (Fig. 8A, left panel). Thus, maintenance of CtBP expression abrogated ARF's induction of apoptosis, suggesting that CtBP degradation/depletion is required for ARF-induced apoptosis in the absence of p53.

To further correlate ARF/CtBP interaction with ARF induction of p53-independent apoptosis, hARF(L50D) was com-

pared with wt hARF for the ability to induce apoptosis. Empty vector, hARF, or hARF(L50D) expression plasmids were transfected into HCT116 p53^{-/-} cells, and cells were analyzed for apoptosis induction by annexin V staining (Fig. 8B, left panel). Similar levels of expression of wt hARF and hARF(L50D) were verified by immunoblotting (Fig. 8B, right panel). As expected, hARF-expressing cells exhibited an increased rate of annexin V positivity (21%), whereas hARF(L50D)-expressing cells exhibited annexin V positivity similar to that observed for cells transfected with empty vector (13% versus 11%) (Fig. 8B, left panel). Thus, the ability of ARF to interact with CtBP correlates with its ability to induce p53-independent apoptosis.

DISCUSSION

ARF exerts tumor suppression functions utilizing both p53-dependent and -independent pathways (27, 48, 57). In this work we have identified CtBP as a putative target for p53-independent ARF functions, where ARF-dependent CtBP

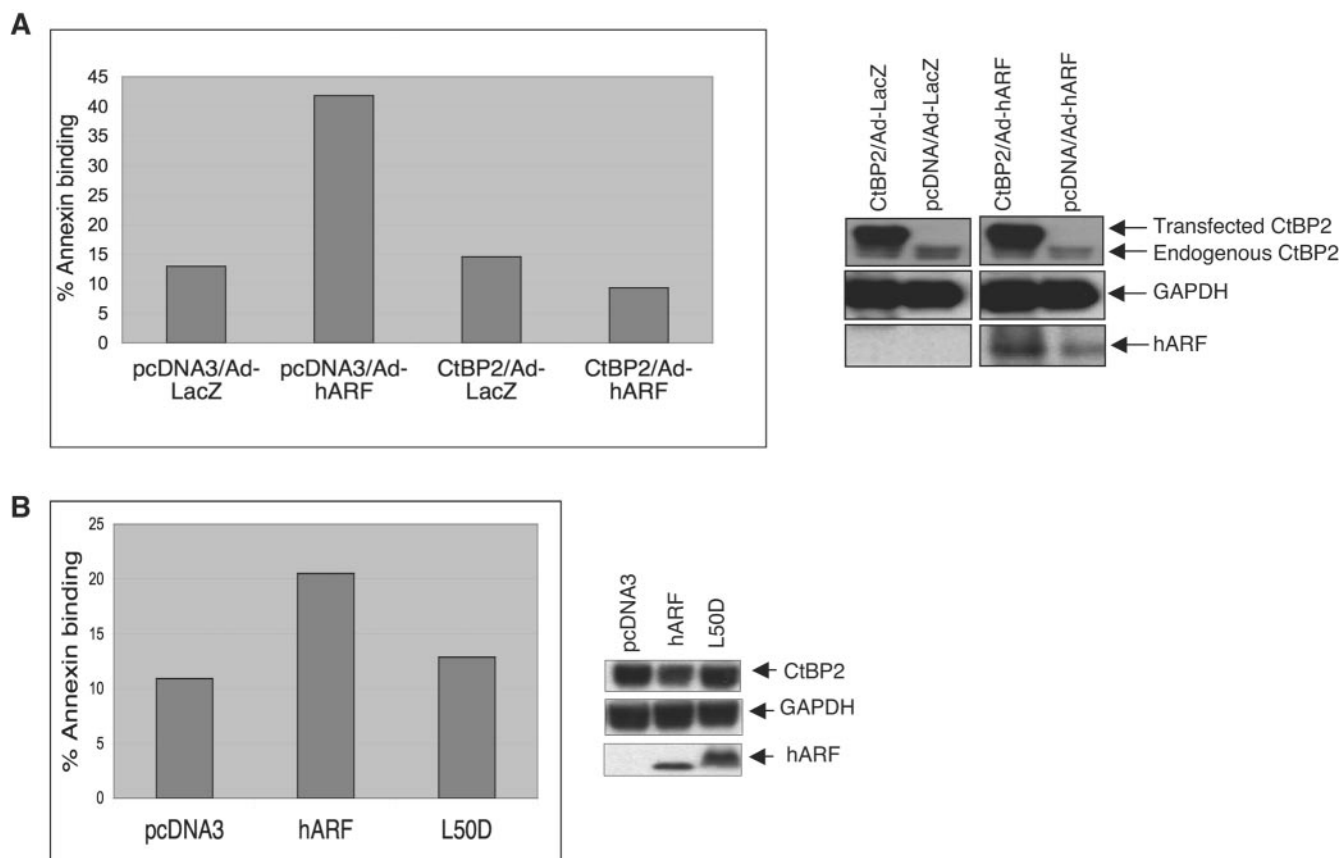


FIG. 8. hARF-induced p53-independent apoptosis requires CtBP2 depletion and interaction. (A) CtBP2 overexpression can revert hARF-induced apoptosis in HCT116 cells. (Left) HCT116 p53^{-/-} cells were transfected with control vector or CtBP2 expression plasmids, and 24 h later, transfected cells were infected with Ad-LacZ or Ad-hARF. Twenty-four hours after infection, the cells were incubated with annexin V-PE along with 7-amino-actinomycin (7-AAD) and analyzed by flow cytometry. Percentages of annexin-positive, viable (7-AAD-negative) cells are displayed. A representative experiment is shown, and similar results were seen in three separate repetitions. (Right) Immunoblots for CtBP2, hARF, and GAPDH expression in the transfected cells. Arrows indicate migration positions of endogenous CtBP2 and exogenous V5-CtBP2. (B) hARF/CtBP2 interaction is required for the induction of apoptosis in p53-null HCT116 cells. (Left) HCT116 p53^{-/-} cells were transfected with control vector, hARF, or L50D mutant expression plasmids, and 72 h after transfection, cells were incubated with annexin V-PE along with 7-AAD and analyzed by flow cytometry. Percentages of annexin-positive, viable (7-AAD-negative) cells are displayed. A representative experiment is shown, and similar results were seen in three separate repetitions. (Right) Immunoblots demonstrating CtBP2, hARF, and GAPDH expression in the transfected cells.

degradation correlated with the ability of ARF to physically interact with CtBP. ARF expression in human colon cancer cells lacking p53 induced efficient apoptosis, as has been noted previously (17). However, apoptosis was also observed after CtBP knockdown alone, suggesting that CtBP lies directly downstream of ARF in its pathway of apoptosis induction. CtBP depletion in ARF-expressing cells via exogenous expression rescued cells from ARF-induced apoptosis, confirming a direct role for CtBP in the apoptosis pathway activated by ARF in the absence of p53.

The mechanism by which ARF destabilizes CtBP is unclear. CtBP2 appeared to be constitutively ubiquitinated and unaffected by ARF expression. Previous work suggests that CtBP1 ubiquitination is directly dependent on S422 phosphorylation (S428 in CtBP2) by HIPK2 upon UV irradiation. If CtBP1 and CtBP2 share a similar mechanism of regulation by the ubiquitin system, our data would suggest that CtBP degradation requires two steps, (i) ubiquitination and (ii) delivery to the proteasome, which may require ARF and possibly additional

factors, such as proteasome adaptors like the human homologs of yeast Dsk2 (hPLIC) and Rad23 (hHR23) proteins (46). We cannot yet account for the difference between our observation of constitutive CtBP2 ubiquitination in HCT116 cells and the previously reported lack of CtBP1 constitutive phosphorylation in monkey COS-7 cells and MEFs. This could be due to technical differences in phosphorylation status of the CtBP2 HIPK2 site in HCT116 cells, experimental approach, other cell type differences, or specific differences between CtBP1 and CtBP2. However, given that UV induces CtBP2 degradation in MEFs only when ARF is present, we propose that CtBP degradation is a two-step process (as outlined above) both in the setting of UV-induced degradation and upon acute human ARF expression, where the addition of UV stress is not required.

As for the identification of the CtBP E3 ubiquitin ligase, one possibility is MDM2 itself, as it interacts with CtBP directly (29). In this case, ARF would not target MDM2 to CtBP, as it binds independently; this is consistent with the observed ARF-

independent constitutive ubiquitination we have observed. Furthermore, MDM2 has already been proposed to serve as a proteasome delivery adaptor for p53, acting after ubiquitination. This activity of MDM2 might be related to its affinity for the proteasome adaptor hHR23 (5). Recent reports also indicate that ARF interacts with a novel hec1 E3 ubiquitin ligase (mule/ARF-BP1) that can ubiquitinate both p53 and mcl-1 (8, 56). Though ARF is reported to inhibit mule/ARF-BP1 E3 activity, further investigation is warranted to determine any possible role for this E3 in the degradation of ARF targets such as CtBP, E2F, and B23/nucleophosmin.

Interestingly, hARF had a much more robust destabilizing influence on CtBP than did mArf, as mArf required concomitant UV stress to induce CtBP degradation. This might account for the absence of a decrease in CtBP2 levels in p53^{-/-} MEFs that express mArf at constitutively high levels. Though the CtBP binding region is well conserved between mArf and hARF, their functional differences might be used as a tool to investigate the mechanism of ARF-mediated CtBP degradation through generation of human/mouse ARF chimeras or comparison of protein interaction profiles.

ARF suppresses spontaneous malignancy in mice, and it is a frequent target for silencing in a variety of human carcinomas (7, 13, 24, 36). The specific cell-autonomous mechanisms by which ARF proteins suppress tumors remain unclear and may depend on cellular and tissue contexts. Both human and mouse ARF are associated with p53-dependent growth arrest, senescence, and apoptosis due to abrogation of MDM2 repression of p53 (47, 57). These activities are absolutely critical for suppression of certain hematopoietic malignancies, such as mouse Eu-Myc transgene-driven B-cell lymphomas and, likely, human T-cell acute lymphoblastic leukemia (12, 14, 37, 43).

However, ARF suppression of epithelial tumors in mice is, at least in part, p53 independent, and the mechanism is unknown (24). Our results and previous work (15, 54) suggest that CtBP maintains a certain antiapoptotic "tone" in cells through repression of proapoptotic gene transcription. Such repression might be abrogated via ARF-induced CtBP degradation, resulting in derepression of such genes. Preliminary data suggest that among apoptosis-specific genes analyzed with a transcription array, the BH3-only protein Bik was upregulated upon either CtBP knockdown or ARF expression (S. Pande, S. Paliwal, and S. R. Grossman, unpublished data).

Specific loss of ARF has been linked to tumor invasiveness and metastasis in a mouse skin cancer model (24). Notably, an antiapoptotic survival signal(s) is necessary for tumor cells to escape their normal microenvironment, invade, and metastasize (1, 45). Suppression of tumor invasion and metastasis by ARF, especially in a setting of p53 inactivation, might therefore ultimately be explained by its ability to induce apoptosis through the inhibitory targeting of CtBP. This model of ARF tumor suppression also suggests the idea that, as a tumor suppressor target, CtBP might act as an oncogene if its expression or activity was dysregulated in cancer cells. Further study of the ARF-CtBP axis in mouse and human cancer will likely yield important insights into mechanisms of tumor progression and provide leads for the therapeutic targeting of this pathway in those tumors where it is dysregulated.

ACKNOWLEDGMENTS

We thank T. Kowalik for high-titer Ad-hARF and Ad-LacZ. Special thanks to members of the Altieri lab for assistance with apoptosis assays and to R. DePinho, D. Altieri, B. Lewis, A. Mercurio, and R. Bates for helpful discussions and critical reading of the manuscript.

S.R.G. was supported by an NCI Howard Temin Award (5KO1-CA89548) and by a Kimmel Scholar Award.

REFERENCES

- Bates, R. C., J. D. Goldsmith, R. E. Bachelder, C. Brown, M. Shibuya, P. Oettgen, and A. M. Mercurio. 2003. Flt-1-dependent survival characterizes the epithelial-mesenchymal transition of colonic organoids. *Curr. Biol.* **13**: 1721–1727.
- Bertwistle, D., M. Sugimoto, and C. J. Sherr. 2004. Physical and functional interactions of the Arf tumor suppressor protein with nucleophosmin/B23. *Mol. Cell. Biol.* **24**:985–996.
- Bothner, B., W. S. Lewis, E. L. DiGiammarino, J. D. Weber, S. J. Bothner, and R. W. Kriwacki. 2001. Defining the molecular basis of Arf and Hdm2 interactions. *J. Mol. Biol.* **314**:263–277.
- Brady, S. N., Y. Yu, L. B. Maggi, Jr., and J. D. Weber. 2004. ARF impedes NPM/B23 shuttling in an Mdm2-sensitive tumor suppressor pathway. *Mol. Cell. Biol.* **24**:9327–9338.
- Brignone, C., K. E. Bradley, A. F. Kisselev, and S. R. Grossman. 2004. A post-ubiquitination role for MDM2 and hHR23A in the p53 degradation pathway. *Oncogene* **23**:4121–4129.
- Bunz, F., A. D., C. Lengauer, T. Waldman, S. Zhou, J. P. Brown, J. M. Sedivy, K. W. Kinzler, and B. Vogelstein. 1998. Requirement for p53 and p21 to sustain G₂ arrest after DNA damage. *Science* **282**:1497–1501.
- Burri, N., P. Shaw, H. Bouzourene, I. Sordat, B. Sordat, M. Gillet, D. Schorderet, F. T. Bosman, and P. Chambert. 2001. Methylation silencing and mutations of the p14ARF and p16INK4a genes in colon cancer. *Lab. Invest.* **81**:217–229.
- Chen, D., N. Kon, M. Li, W. Zhang, J. Qin, and W. Gu. 2005. ARF-BP1/Mule is a critical mediator of the ARF tumor suppressor. *Cell* **121**:1071–1083.
- Chinnadurai, G. 2002. CtBP, an unconventional transcriptional corepressor in development and oncogenesis. *Mol. Cell* **9**:213–224.
- Datta, A., A. Nag, W. Pan, N. Hay, A. L. Gartel, O. Colamonici, Y. Mori, and P. Raychaudhuri. 2004. Myc-ARF (alternate reading frame) interaction inhibits the functions of Myc. *J. Biol. Chem.* **279**:36698–36707.
- Datta, A., A. Nag, and P. Raychaudhuri. 2002. Differential regulation of E2F1, DP1, and the E2F1/DP1 complex by ARF. *Mol. Cell. Biol.* **22**:8398–8408.
- Eischen, C. M., J. D. Weber, M. F. Roussel, C. J. Sherr, and J. L. Cleveland. 1999. Disruption of the ARF-Mdm2-p53 tumor suppressor pathway in Myc-induced lymphomagenesis. *Genes Dev.* **13**:2658–2669.
- Esteller, M., S. Tortola, M. Toyota, G. Capella, M. A. Peinado, S. B. Baylin, and J. G. Herman. 2000. Hypermethylation-associated inactivation of p14^{ARF} is independent of p16^{INK4a} methylation and p53 mutational status. *Cancer Res.* **60**:129–133.
- Gardie, B., J.-M. Cayuela, S. Martini, and F. Sigaux. 1998. Genomic alterations of the p19^{ARF} encoding exons in T-cell acute lymphoblastic leukemia. *Blood* **91**:1016–1020.
- Grooteclaes, M., Q. Deveraux, J. Hildebrand, Q. Zhang, R. H. Goodman, and S. M. Frisch. 2003. C-terminal-binding protein corepresses epithelial and proapoptotic gene expression programs. *Proc. Natl. Acad. Sci. USA* **100**:4568–4573.
- Harris, S. L., and A. J. Levine. 2005. The p53 pathway: positive and negative feedback loops. *Oncogene* **24**:2899–2908.
- Hemmati, P. G., B. Gillissen, C. von Haefen, J. Wendt, L. Starck, D. Guner, B. Dorken, and P. T. Daniel. 2002. Adenovirus-mediated overexpression of p14^{ARF} induces p53 and Bax-independent apoptosis. *Oncogene* **21**:3149–3161.
- Itahana, K., K. P. Bhat, A. Jin, Y. Itahana, D. Hawke, R. Kobayashi, and Y. Zhang. 2003. Tumor suppressor ARF degrades B23, a nucleolar protein involved in ribosome biogenesis and cell proliferation. *Mol. Cell* **12**:1151–1164.
- Jones, S. N., A. E. Roe, L. A. Donehower, and A. Bradley. 1995. Rescue of embryonic lethality in Mdm2-deficient mice by absence of p53. *Nature* **378**: 206–208.
- Kabuyama, Y., M. K. Homma, M. Sekimata, and Y. Homma. 2001. Wave-length-specific activation of MAP kinase family proteins by monochromatic UV irradiation. *Photochem. Photobiol.* **73**:147–152.
- Kamijo, T., S. Bodner, E. van de Kamp, D. H. Randle, and C. J. Sherr. 1999. Tumor spectrum in ARF-deficient mice. *Cancer Res.* **59**:2217–2222.
- Kamijo, T., F. Zindy, M. F. Roussel, D. E. Quelle, J. R. Downing, R. A. Ashmun, G. Grosfeld, and C. J. Sherr. 1997. Tumor suppression at the mouse INK4a locus mediated by the alternative reading frame product p19ARF. *Cell* **91**:649–659.

23. Katsanis, N., and E. M. Fisher. 1998. A novel C-terminal binding protein (CTBP2) is closely related to CTBP1, an adenovirus E1A-binding protein, and maps to human chromosome 21q21.3. *Genomics* **47**:294–299.
24. Kelly-Spratt, K. S., K. E. Gurley, Y. Yasui, and C. J. Kemp. 2004. p19^{ARF} suppresses growth, progression, and metastasis of Hras-driven carcinomas through p53-dependent and -independent pathways. *PLoS Biol.* **2**:E242.
25. Korgaonkar, C., J. Hagen, V. Tompkins, A. A. Frazier, C. Allamargot, F. W. Quelle, and D. E. Quelle. 2005. Nucleophosmin (B23) targets ARF to nucleoli and inhibits its function. *Mol. Cell. Biol.* **25**:1258–1271.
26. Lindstrom, M. S., U. Klangby, R. Inoue, P. Pisa, K. G. Wiman, and C. E. Asker. 2000. Immunolocalization of human p14^{ARF} to the granular component of the interphase nucleolus. *Exp. Cell Res.* **256**:400–410.
27. Lowe, S. W., and C. J. Sherr. 2003. Tumor suppression by Ink4a/Arf: progress and puzzles. *Curr. Opin. Genet. Dev.* **13**:77–83.
28. Martelli, F., T. Hamilton, D. P. Silver, N. E. Sharpless, N. Bardeesy, M. Rokas, R. A. DePinho, D. M. Livingston, and S. R. Grossman. 2001. p19^{ARF} targets certain E2F species for degradation. *Proc. Natl. Acad. Sci. USA* **98**:4455–4460.
29. Mirnezami, A. H., S. J. Campbell, M. Darley, J. N. Primrose, P. W. Johnson, and J. P. Blaydes. 2003. Hdm2 recruits a hypoxia-sensitive corepressor to negatively regulate p53-dependent transcription. *Curr. Biol.* **13**:1234–1239.
30. Montes de Oca Luna, R., D. S. Wagner, and G. Lozano. 1995. Rescue of early embryonic lethality in *mdm2*-deficient mice by deletion of *p53*. *Nature* **378**:203–206.
31. Moore, L., S. Venkatachalam, H. Vogel, J. C. Watt, C. L. Wu, H. Steinman, S. N. Jones, and L. A. Donehower. 2003. Cooperativity of p19^{ARF}, Mdm2, and p53 in murine tumorigenesis. *Oncogene* **22**:7831–7837.
32. Pelech, S. L., B. B. Olwin, and E. G. Krebs. 1986. Fibroblast growth factor treatment of Swiss 3T3 cells activates a subunit S6 kinase that phosphorylates a synthetic peptide substrate. *Proc. Natl. Acad. Sci. USA* **83**:5968–5972.
33. Qi, Y., M. A. Gregory, Z. Li, J. P. Brousal, K. West, and S. R. Hann. 2004. p19^{ARF} directly and differentially controls the functions of c-Myc independently of p53. *Nature* **431**:712–717.
34. Quelle, D. E., F. Zindy, R. A. Ashmun, and C. J. Sherr. 1995. Alternative reading frames of the INK4a tumor suppressor gene encode two unrelated proteins capable of inducing cell cycle arrest. *Cell* **83**:993–1000.
35. Rozenblum, E., M. Schutte, M. Goggins, S. A. Hahn, S. Panzer, M. Zahurak, S. N. Goodman, T. A. Sohn, R. H. Hruban, C. J. Yeo, and S. E. Kern. 1997. Tumor-suppressive pathways in pancreatic carcinoma. *Cancer Res.* **57**:1731–1734.
36. Sato, F., N. Harpaz, D. Shibata, Y. Xu, J. Yin, Y. Mori, T.-T. Zou, S. Wang, K. Desai, A. Leytin, F. M. Selaru, J. M. Abraham, and S. J. Meltzer. 2002. Hypermethylation of the p14^{ARF} gene in ulcerative colitis-associated colorectal carcinogenesis. *Cancer Res.* **62**:1148–1151.
37. Schmitt, C. A., M. E. McCurrach, E. de Stanchina, R. R. Wallace-Brodeur, and S. W. Lowe. 1999. INK4a/ARF mutations accelerate lymphomagenesis and promote chemoresistance by disabling p53. *Genes Dev.* **13**:2670–2677.
38. Sharpless, N. E. 2005. INK4a/ARF: a multifunctional tumor suppressor locus. *Mutat. Res.* **576**:22–38.
39. Sharpless, N. E., M. R. Ramsey, P. Balasubramanian, D. H. Castrillon, and R. A. DePinho. 2004. The differential impact of p16^{INK4a} or p19^{ARF} deficiency on cell growth and tumorigenesis. *Oncogene* **23**:379–385.
40. Sherr, C. J., and J. D. Weber. 2000. The ARF/p53 pathway. *Curr. Opin. Genet. Dev.* **10**:94–99.
41. Sugimoto, M., M. L. Kuo, M. F. Roussel, and C. J. Sherr. 2003. Nucleolar Arf tumor suppressor inhibits ribosomal RNA processing. *Mol. Cell* **11**:415–424.
42. Tago, K., S. Chiocca, and C. J. Sherr. 2005. Sumoylation induced by the Arf tumor suppressor: a p53-independent function. *Proc. Natl. Acad. Sci. USA* **102**:7689–7694.
43. Takemoto, S., R. Trovato, A. Cereseto, C. Nicot, T. Kislyakova, L. Casareto, T. Waldmann, G. Torelli, and G. Franchini. 2000. p53 stabilization and functional impairment in the absence of genetic mutation or the alteration of the p14^{ARF}-MDM2 loop in ex vivo and cultured adult T-cell leukemia/lymphoma cells. *Blood* **95**:3939–3944.
44. Tao, W., and A. J. Levine. 1999. p19^{ARF} stabilizes p53 by blocking nucleocytoplasmic shuttling of Mdm2. *Proc. Natl. Acad. Sci. USA* **96**:6937–6941.
45. Thiery, J. P. 2002. Epithelial-mesenchymal transitions in tumour progression. *Nat. Rev. Cancer* **2**:442–454.
46. Verma, R., R. Oania, J. Graumann, and R. J. Deshaies. 2004. Multiubiquitin chain receptors define a layer of substrate selectivity in the ubiquitin-proteasome system. *Cell* **118**:99–110.
47. Weber, H. O., T. Samuel, P. Rauch, and J. O. Funk. 2002. Human p14^{ARF}-mediated cell cycle arrest strictly depends on intact p53 signaling pathways. *Oncogene* **21**:3207–3212.
48. Weber, J. D., J. R. Jeffers, J. E. Rehg, D. H. Randle, G. Lozano, M. F. Roussel, C. J. Sherr, and G. P. Zambetti. 2000. p53-independent functions of the p19^{ARF} tumor suppressor. *Genes Dev.* **14**:2358–2365.
49. Weber, J. D., M.-L. Kuo, B. Bothner, E. L. DiGiammarino, R. W. Kriwacki, M. F. Roussel, and C. J. Sherr. 2000. Cooperative signals governing ARF-Mdm2 interaction and nucleolar localization of the complex. *Mol. Cell. Biol.* **20**:2517–2528.
50. Weber, J. D., L. J. Taylor, M. F. Roussel, C. J. Sherr, and D. Bar-Sagi. 1999. Nucleolar Arf sequesters Mdm2 and activates p53. *Nat. Cell Biol.* **1**:20–26.
51. Xirodimas, D. P., J. Chisholm, J. M. Desterro, D. P. Lane, and R. T. Hay. 2002. P14^{ARF} promotes accumulation of SUMO-1 conjugated (H)Mdm2. *FEBS Lett.* **528**:207–211.
52. Yarbrough, W. G., M. Bessho, A. Zanation, J. E. Bisi, and Y. Xiong. 2002. Human tumor suppressor ARF impedes S-phase progression independent of p53. *Cancer Res.* **62**:1171–1177.
53. Zhang, Q., A. Nottke, and R. H. Goodman. 2005. Homeodomain-interacting protein kinase-2 mediates CtBP phosphorylation and degradation in UV-triggered apoptosis. *Proc. Natl. Acad. Sci. USA* **102**:2802–2807.
54. Zhang, Q., Y. Yoshimatsu, J. Hildebrand, S. M. Frisch, and R. H. Goodman. 2003. Homeodomain interacting protein kinase 2 promotes apoptosis by downregulating the transcriptional corepressor CtBP. *Cell* **115**:177–186.
55. Zhang, Y., and Y. Xiong. 1999. Mutations in human ARF exon 2 disrupt its nucleolar localization and impair its ability to block nuclear export of MDM2 and p53. *Mol. Cell* **3**:579–591.
56. Zhong, Q., W. Gao, F. Du, and X. Wang. 2005. Mule/ARF-BP1, a BH3-only E3 ubiquitin ligase, catalyzes the polyubiquitination of Mcl-1 and regulates apoptosis. *Cell* **121**:1085–1095.
57. Zindy, F., C. M. Eischen, D. H. Randle, T. Kamijo, J. L. Cleveland, C. J. Sherr, and M. F. Roussel. 1998. Myc signaling via the ARF tumor suppressor regulates p53-dependent apoptosis and immortalization. *Genes Dev.* **12**:2424–2433.